Advanced O-band transmission using maximum likelihood sequence estimation

Hiroki Taniguchi(1), Shuto Yamamoto(1), Masanori Nakamura(1), Akira Masuda(1), Yoshiaki Kisaka(1), Shigeru Kanazawa(2), Hirotaka Nakamura(2)

(1) NTT Network Innovation Laboratories, NTT Corporation, hiroki.taniguchi.ys@hco.ntt.co.jp
(2) NTT Device Innovation Center, NTT Corporation

Abstract. *We discuss advanced maximum likelihood sequence estimation methods for short reach IM-DD transmission, which include reducing complexity of Viterbi algorithm and improving the decoding performance with precise emulation of nonlinear responses in transmission systems. We also present transmission experiments over 200-Gbps/lane using our proposed methods. ©2022 The Author(s)*

Introduction

Traffic growth in datacentre networks remains a major challenge. Ethernet is deployed in data-centre networks to economically provide high-capacity short-reach transmission by increasing the modulation rate, number of symbol levels, and number of wavelength channels in intensity-modulated direct detection (IM-DD) systems. A task force meeting of the IEEE P802.3df project is underway for the next generation 400GbE [1]. To achieve 800GbE, 200Gbps/lane, 4-lambda wavelength-division multiplexing (WDM) is planned as one of the objectives of IEEE P802.3df.

Large inter-symbol interference (ISI), which is caused by severe bandwidth limitations and wavelength dispersion in high-speed IM-DD transmission, has becomes a critical issue. It is important to remove ISI without noise enhancement by the equalization process, and several methods have been reported. For example, nonlinear-differential-coded pulse amplitude modulation (PAM) and partial response encoding have been studied as spectral shaping techniques at the transmitter side digital signal processing (DSP) [2-5]. Tomlinson-Harashima precoding and discrete multi-tone have also been studied as methods for maximizing the use of a priori transmission-function information [6-8]. The decision feedback equalizer (DFE) and maximum likelihood sequence estimation (MLSE) have been studied as techniques for receiver-side DSP [9, 10].

MLSE unlike transmitter side DSP techniques, does not require modulation-format changes and prior transfer-function information, and does not cause error propagation as DFE does. However, it is relatively computationally complex compared with other receiver-side DSP methods, and its effectiveness is reduced in transmission systems with transfer functions that have non-linear responses, as is the case with other DSP methods.

We focus on our previously proposed methods for reducing the complexity and improving estimation accuracy of MLSE [11-20]. We also discuss our experiments involving O-band transmission over 200-Gbps/lane using our MLSE methods and present the results.

Improvement aspects of MLSE

In this section, we explain the concept of MLSE and the Viterbi algorithm, and point out two problems with MLSE.

Figure 1 shows the concept of a transmission system and a receiver-side DSP using MLSE with the Viterbi algorithm. The Viterbi algorithm in MLSE prepares candidate sequences $\boldsymbol{C}$ that represent all possible parts of the transmitted signal sequence $\boldsymbol{x_n}$. The number of symbols in this candidate sequence corresponds to the memory length l of the estimated transfer function of the transmission system. The number of candidate sequences is expressed as m^l using the number of symbol types m and l. To obtain a decision of the received signal, the path metrics of the trellis diagram are calculated. Path metrics are the sum of the metrics of all the branches that constitute each path. A branch metric is the square of the difference between the received signal and estimated received signal.

The first improvement in MLSE is in the calculation amount. The Viterbi algorithm does not sequentially increase the number of path metrics by truncating paths with larger metrics. However, the branch metrics corresponding to all

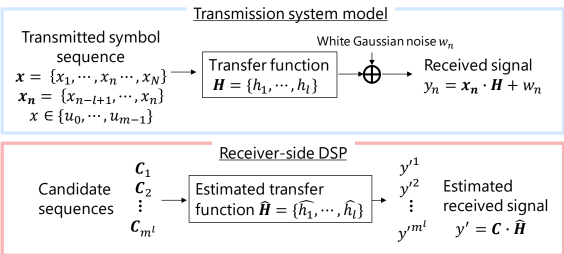

Fig. 1: Concept of transmission system and MLSE.

the candidate sequences need to be calculated m^l times for each symbol. This indicates that reducing the number of candidate sequences represented by m and l is significantly effective in reducing computational complexity. A way to reduce m in the Viterbi algorithm is MLSE with trellis-path limitation described in the next section. Another way to reduce l in the Viterbi algorithm is MLSE with decision feedback, which is described in a later section.

The second improvement in MLSE is the accuracy of transfer-function estimation. As shown in Figure 1, in the conventional MLSE method, the estimated transfer function $\hat{\boldsymbol{H}}$ is represented by linear coefficients only. If the transfer function $\boldsymbol{H}$ had only linear elements, the receiver-side DSP would be able to estimate the transfer function correctly. However, the response of devices used in actual transmission systems is not always guaranteed to be linear, and especially in low-cost transmission systems, it is important to consider that the system consists of devices with non-linear responses. Therefore, it is effective to enable estimation of transfer functions that include non-linear responses to improve estimation accuracy. MLSE for non-linear channel estimation as a method for achieving the above is described late in the paper.

MLSE with trellis-path limitation

To reduce the number of candidate sequences, we previously proposed a trellis-path limitation MLSE method (TL-MLSE), as shown in Figure 2 [11]. The received signal sequence is input to a channel shortening filter (CSF) and down-sampled from T/2-space to T-space. As a result, the impulse response of the CSF output is compressed in the time direction. The candidate sequences are input to a desired impulse response filter (DIRF), which represents the estimated transfer function. In the conventional Viterbi algorithm, candidate sequences need to be generated for all transmission patterns, and the branch metrics corresponding to all candidate sequences need to be calculated. Therefore, this method uses the coarse decision result from prior linear equalization (LEQ) to limit the transmission patterns to be considered in the Viterbi algorithm. When only the symbols represented by the coarse decision result and the adjacent symbols are considered, the number of candidate sequences is suppressed to 3^l.

Figure 3 shows the experimental results of the tap-length dependencies on LEQ and CSF in (a) PAM-8 225-Gbps (75-GBaud) 10-km transmission and (b) PAM-8 255-Gbps (85-GBaud) 10-km transmission in the O-band for

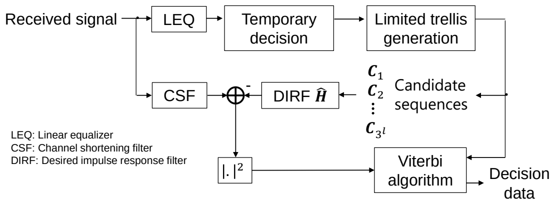

Fig. 2: Block diagram of TL-MLSE. (LEQ: Linear equalizer, CSF: Channel shortening filter, DIRF: Desired impulse response filter)

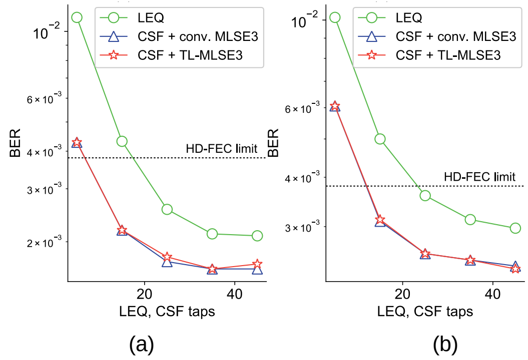

Fig. 3: Transmission performance for (a) 225-Gbps 10-km transmission and (b) 255-Gbps 10-km transmission for LEQ (circles), conventional MLSE (triangles) and TL-MLSE (stars).

LEQ only and the conventional MLSE and our TL-MLSE methods with the 3-memory DIRF. Regardless of the tap length, the performance of TL-MLSE is almost same as that of the conventional MLSE method and improved compared with LEQ.

A method to further reduce the number of candidate sequences is proposed in [21]. This method uses only two symbol levels, which are above and below the output of the linear filter in LEQ to generate candidate sequences; thus, the number of candidate sequences become 2^l.

MLSE based on nonlinear filter

To estimate the non-linear channel response, we proposed a non-linear MLSE (NL-MLSE) based on Volterra series expansion [12–20]. Figure 4 shows a block diagram of NL-MLSE. The output of an l–memory DIRF with 3rd order Volterra series expansion is expressed as

$$\boldsymbol{f}(\boldsymbol{x}_1, \cdots, \boldsymbol{x}_l) = \sum_{a=1}^{l} \boldsymbol{h}_a \boldsymbol{x}_a + \sum_{a=1}^{l} \sum_{b=1}^{l} \boldsymbol{h}_{ab} \boldsymbol{x}_a \boldsymbol{x}_b + \sum_{a=1}^{l} \sum_{b=1}^{l} \sum_{c=1}^{l} \boldsymbol{h}_{abc} \boldsymbol{x}_a \boldsymbol{x}_b \boldsymbol{x}_c \,, \qquad (1)$$

where $(x_1, \cdots, x_l)$ is a candidate sequence such as the input of the DIRF, and $(h_{1\sim l}, h_{11\sim ll}, h_{111\sim lll})$

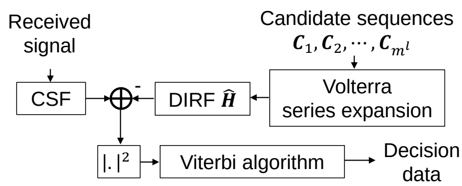

Fig. 4: Block diagram of NL-MLSE.

are kernels of the Volterra series expansion. By removing the kernels that have the least impact on the DIRF output, i.e., the kernels with the small values the amount of non-linear calculations can be reduced while minimizing performance degradation [20].

MLSE using decision feedback

The other of MLSE methods is for reducing the computational complexity of MLSE is to apply a decision feedback function to MLSE (DF-MLSE) [20]. Figure 5 shows a block diagram of DF-MLSE with Volterra series expansion for non-linear channel estimation (DF-NL-MLSE). Generally, the inputs of the DIRF are generated as candidate sequences. To reduce the number of candidate sequences while suppressing MLSE-performance degradation, some of the decision results are fed back to the input of the DIRF. This increases the length of the input sequences to the DIRF without changing the number of candidate sequences and improves the accuracy of the metrics in the Viterbi algorithm. If the trace-back delay is too long for the desired feedback timing, the decision result is determined without trace back. For example, if the length of the candidate sequences is three symbols and the decision feedback is two symbols, the output of the DIRF with 3rd order Volterra series expansion can be expressed as

$$\boldsymbol{f}\left(\hat{\boldsymbol{d}}_{-4}, \hat{\boldsymbol{d}}_{-3}, \boldsymbol{c}_{-2}, \boldsymbol{c}_{-1}, \boldsymbol{c}_{0}\right) = \sum_{a=-4}^{-3} \boldsymbol{p}_a \hat{\boldsymbol{d}}_a + \sum_{a=-2}^{0} \boldsymbol{q}_a \boldsymbol{c}_a + \sum_{a=-2}^{0} \sum_{b=-2}^{0} \boldsymbol{r}_{ab} \boldsymbol{c}_a \boldsymbol{c}_b + \sum_{a=-2}^{0} \sum_{b=-2}^{0} \sum_{c=-2}^{0} \boldsymbol{s}_{abc} \boldsymbol{c}_a \boldsymbol{c}_b \boldsymbol{c}_c \,, \quad (2)$$

where $(\hat{d}_{-4}, \hat{d}_{-3})$ are decision-feedback symbols, (c_{-2}, c_{-1}, c_0) is a candidate sequence, and ($p_{-4,-3}$, $q_{-2\sim 0}$, $r_{-2-2\sim 00}$, $s_{-2-2-2\sim 000}$) are taps and kernels of the DIRF. For the PAM-4 symbol, the number of candidate sequences in the above case is 64, which reduces the number of candidate sequences to one-sixteenth those required when compared with inputting sequences of length 5 with no decision feedback.

We experimentally evaluate the performance of DF-NL-MLSE in a 4-ch high-baud-rate PAM-4 transmission. The electrical 224-Gbps PAM-4 signals are modulated to 4-ch WDM optical signals by a 4-λ LAN-WDM TOSA consisting of electro-absorptive modulated lasers with integrated semiconductor optical amplifiers and a wavelength multiplexer [22].

Figure 6 shows the results of 112-GBd PAM-4 in 2-km transmission for all WDM channels. The demodulation by LEQ and the conventional MLSE method could not achieve a bit error rate (BER) below 3.8×10^{-3}, which corresponds to 7% overhead hard-decision forward error correction (HD-FEC) limit in all wavelength channels. The NL-MLSE and linear MLSE with decision feedback (DF-MLSE) could not reach the HD-FEC limit in some wavelength channels. However, DF-NL-MLSE was below the HD-FEC limit in all wavelength channels.

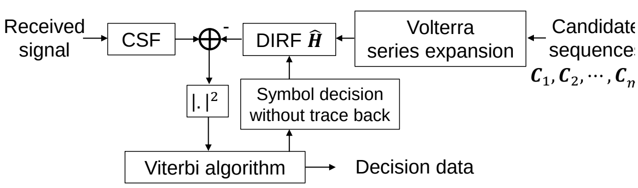

Fig. 5: Block diagram of DF-MLSE with Volterra series expansion.

Tab. 1: Comparison of calculation quantities. (PAM-4 signal in transfer function memory length $\boldsymbol{l}$ decision feedback M.)

Conv. MLSE	TL-MLSE	NL-MLSE	DF-MLSE
1	0.75^ $\boldsymbol{l}$	1	0.25^M

Comparison of calculation quantities

To confirm the calculation reduction of the above MLSE methods, Table 1 shows the ratio of the number of candidate sequences assuming a PAM-4 signal with a transfer function memory length $\boldsymbol{l}$ and decision feedback M. The larger $\boldsymbol{l}$ for TL-MLSE and M for DF-MLSE, the greater reduction in the amount of calculation.

Conclusions

We described our MLSE methods for improving the accuracy of non-linear channel-response estimation and reducing computational complexity in high-speed IM-DD systems. The experimental results of over 200-Gbps/lane O-band transmission using these MLSE methods were also presented.

Acknowledgements

We would like to thank Furukawa Electric Co., Ltd. for contributing the 4-λ LAN-WDM TOSA.

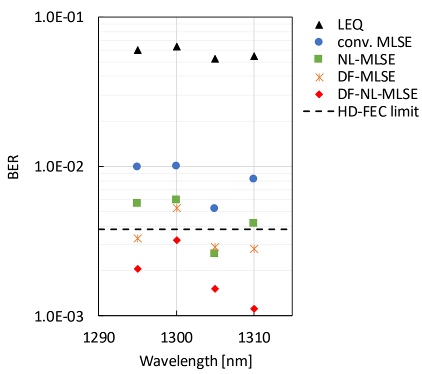

Fig. 6: 224-Gbps/λ 4-ch LAN-WDM PAM-4 performance in 2-km transmission.

References

[1] IEEE P802.3df 200 Gb/s, 400 Gb/s, 800 Gb/s, and 1.6 Tb/s Ethernet Task Force, https://www.ieee802.org/3/df/index.html, accessed on 2 June 2022.

[2] S. Yamamoto, H. Taniguchi, M. Nakamura and Y. Kisaka, "O-Band 10-km PAM Transmission Using Nonlinear-Spectrum-Shaping Encoder and Transition-Likelihood-Based Decoder with Symbol- and Likelihood-Domain Feedbacks," 2021 European Conference on Optical Communication (ECOC), 2021, pp. 1-4, doi: 10.1109/ECOC52684.2021.9605867.

[3] S. Yamamoto, H. Taniguchi, M. Nakamura and Y. Kisaka, "Nonlinear Differential Coding for Spectral Shaping of PAM Signal in High-Baudrate Short-Reach Optical Transmission," in *Journal of Lightwave Technology*, vol. 39, no. 4, pp. 1064-1071, 15 Feb.15, 2021, doi: 10.1109/JLT.2020.3030095.

[4] Q. Hu et al., "Ultrahigh-Net-Bitrate 363 Gbit/s PAM-8 and 279 Gbit/s Polybinary Optical Transmission Using Plasmonic Mach-Zehnder Modulator," in Journal of Lightwave Technology, vol. 40, no. 10, pp. 3338-3346, 15 May15, 2022, doi: 10.1109/JLT.2022.3172246.

[5] M. S. -B. Hossain et al., "Partial Response O-band EML Transmission Beyond 300-GBd with a 128/256 GSa/s DAC," 2022 Optical Fiber Communications Conference and Exhibition (OFC), 2022, pp. 1-3.

[6] N. Kikuchi and R. Hirai, "Application of Generalized THP for Arbitrary PAM Level Design in Short-Reach IM/DD Signalling," 2021 European Conference on Optical Communication (ECOC), 2021, pp. 1-3, doi: 10.1109/ECOC52684.2021.9605883.

[7] Q. Hu, M. Chagnon, K. Schuh, F. Buchali and H. Bülow, "High data rate Tomlinson-Harashima-precoding-based PAM transmission," 45th European Conference on Optical Communication (ECOC 2019), 2019, pp. 1-4, doi: 10.1049/cp.2019.0869.

[8] H. Yamazaki et al., "300-Gbps Discrete Multi-tone Transmission Using Digital-Preprocessed Analog-Multiplexed DAC with Halved Clock Frequency and Suppressed Image," ECOC 2016 - Post Deadline Paper; 42nd European Conference on Optical Communication, 2016, pp. 1-3.

[9] M. S. -B. Hossain et al., "Transmission Beyond 200 Gbit/s With IM/DD System for Campus and Intra-Datacenter Network Applications," in IEEE Photonics Technology Letters, vol. 33, no. 5, pp. 263-266, 1 March1, 2021, doi: 10.1109/LPT.2021.3056005.

[10] W. Wang et al., "Demonstration of 214Gbps Per Lane IM/DD PAM-4 Transmission using O-Band 35GHz-Class EML with Advanced MLSE and KP4-FEC," 2020 Optical Fiber Communications Conference and Exhibition (OFC), 2020, pp. 1-3.

[11] H. Taniguchi et al., "255-Gb/s PAM8 O-band Transmission through 10-km SMF using simplified MLSE based on Trellis-path Limitation," IEICE Tech. Rep., vol. 119, no. 366, OCS2019-65, pp. 1-6, Jan. 2020.

[12] A. Masuda, S. Yamamoto, H. Taniguchi and M. Fukutoku, "Achievement of 90-Gbaud PAM-4 with MLSE Based on 2nd Order Volterra Filter and 2.88-Tb/s O-band Transmission Using 4-λ LAN-WDM and 4-Core Fiber SDM," 2018 Optical Fiber Communications Conference and Exposition (OFC), 2018, pp. 1-3.

[13] A. Masuda, H. Taniguchi, S. Yamamoto, Y. Ogiso and M. Fukutoku, "96-Gbaud PAM-4 Transmission with 1 sample/symbol under 22-GHz Bandwidth Limitation Using NL-MLSE Based on Third-Order Volterra Filter," 2018 European Conference on Optical Communication (ECOC), 2018, pp. 1-3, doi: 10.1109/ECOC.2018.8535509.

[14] H. Taniguchi, S. Yamamoto, A. Masuda and M. Fukutoku, "Achievement of 186-Gb/s PAM-4 under 20.5-GHz bandwidth limitation using MLSE based on 2nd order Volterra filter," 2018 23rd Opto-Electronics and Communications Conference (OECC), 2018, pp. 1-2, doi: 10.1109/OECC.2018.8730055.

[15] A. Masuda, S. Yamamoto, H. Taniguchi, M. Nakamura and Y. Kisaka, "255-Gbps PAM-8 Transmission under 20-GHz Bandwidth Limitation using NL-MLSE Based on Volterra Filter," 2019 Optical Fiber Communications Conference and Exhibition (OFC), 2019, pp. 1-3.

[16] S. Yamamoto, H. Taniguchi, M. Nakamura and Y. Kisaka, "O-band Transmission of 255-Gb/s PAM8 Signal through 10-km SMF Using MLSE Based on Nonlinear Channel Estimation," 2019 24th OptoElectronics and Communications Conference (OECC) and 2019 International Conference on Photonics in Switching and Computing (PSC), 2019, pp. 1-3, doi: 10.23919/PS.2019.8817769.

[17] H. Taniguchi et al., "84-GBaud/λ PAM-4 Transmission over 20-km using 4-λ LAN-WDM TOSA and ROSA with MLSE Based on Nonlinear Channel Estimation," 2020 Optical Fiber Communications Conference and Exhibition (OFC), 2020, pp. 1-3.

[18] H. Taniguchi et al., "225-Gbps/λ PAM-8 Transmission over 2-km using 4-λ LAN-WDM TOSA with MLSE Based on Nonlinear Channel Estimation," 2020 Opto-Electronics and Communications Conference (OECC), 2020, pp. 1-3, doi: 10.1109/OECC48412.2020.9273573.

[19] H. Taniguchi, S. Yamamoto, M. Nakamura and Y. Kisaka, "255-Gbps PAM-8 O-band Transmission through 10-km SMF under 14-GHz Bandwidth Limitation Using MLSE Based on Nonlinear Channel Estimation with Cutdown Volterra Kernels," 2020 European Conference on Optical Communications (ECOC), 2020, pp. 1-3, doi: 10.1109/ECOC48923.2020.9333349.

[20] H. Taniguchi et al., "800-Gbps PAM-4 O-band Transmission through 2-km SMF using 4λ LAN-WDM TOSA with MLSE Based on Nonlinear Channel Estimation and Decision Feedback," 2021 European Conference on Optical Communication (ECOC), 2021, pp. 1-4, doi: 10.1109/ECOC52684.2021.9606080.

[21] Yukui Yu, Yi Che, Tianwai Bo, Daeho Kim, and Hoon Kim, "Reduced-state MLSE for an IM/DD system using PAM modulation," Opt. Express 28, 38505-38515 (2020).

[22] S. Kanazawa et al., "High Output Power and Compact LAN-WDM EADFB Laser TOSA for 4 × 100-Gbit/s/λ 40-km Fiber-Amplifier-Less Transmission," 2020 Optical Fiber Communications Conference and Exhibition (OFC), 2020, pp. 1-3.